An Improved COLD Approach for Monitoring Construction Dynamics Using HLS and LULC Data: A Case Study in the New Capital of Egypt

Mahmoud Abdallah[1, 2, 4], Eslam Ali[3, 5], Xiaoli Ding[1, 2], Songbo Wu[1, 2]

[1] Department of Land Surveying and Geo-Informatics, The Hong Kong Polytechnic University, Hong Kong, China - mahmoud.abdallah@connect.polyu.hk; xl.ding@polyu.edu.hk; songbo.wu@connect.polyu.hk
[2] Research Institution for Land and Space, The Hong Kong Polytechnic University, Hong Kong, China
[3] Department of Building and Real Estate, The Hong Kong Polytechnic University, Hong Kong, China - eslam.saleh@polyu.edu.hk
[4] Public Works Department, Mansoura University, Mansoura, Egypt
[5] Public Works Department, Cairo University, Giza, Egypt

KEYWORDS: Construction Change; HLS, LULC; COLD; Time Series.

Abstract

Accurate change detection is essential for understanding land disturbances. The Continuous Monitoring of Land Disturbances (COLD) algorithm is a widely used method for detecting rapid ground changes using Harmonized Landsat and Sentinel (HLS) data. Despite its advancements, change detection accuracy is often limited by frequent ground alterations, such as large-scale construction during urbanization. This study proposes an improved COLD algorithm that integrates land disturbances identified by COLD with publicly available land use/land cover (LULC) maps from Esri, covering the period from 2017 to 2024, to map and quantify construction activities. To evaluate the performance of the proposed method, this study takes the new capital of Egypt as the study area, which is experiencing a surge in national infrastructure projects. We focused on tracking construction dynamics from 2016 to the present. The spatiotemporal detection of land disturbances uses the COLD algorithm with a dataset of 559 images from Harmonized Landsat and Sentinel missions. The identified COLD breaks correspond to transition periods, capturing changes from July of one year to July of the next. Then, two distinct overlapping analyses were performed: first, we aligned the COLD-detected disturbances with the LULC maps of the same year; second, we overlaid the LULC maps of the following year with the COLD results. While both methods yielded similar insights, the latter approach identified a more extensive area classified as undergoing construction, providing a more accurate depiction of progressive development. We validated the results by visually comparing detected construction activities over time and cross-referencing with historical satellite imagery from Google Earth. This approach has proven effective for monitoring and mapping construction changes and holds potential for application in other regions with available LULC maps.

1. Introduction

Land disturbance refers to events that rapidly alter the structure, composition, or function of ecosystems. While natural events such as wildfires, floods, and earthquakes can drive these changes, anthropogenic activities, particularly deforestation, mining, and construction, have become the dominant sources of land disturbance in recent decades. With over 55% of the global population now residing in urban areas (United Nations, 2022), rapid urbanization has significantly accelerated land-use transformations, leading to both local and global environmental impacts (Winkler et al., 2021). A notable consequence of this urban expansion is that construction-induced disturbances disrupt ecological processes such as the carbon cycle, reduce biodiversity, and exacerbate climate change by altering surface properties like albedo and thermal characteristics (Friedl et al., 2002). These far-reaching impacts underscore the need to continuously monitor land disturbances to support sustainable urban development and bolster climate resilience.

Satellite remote sensing has become a critical tool for monitoring land disturbances because it provides consistent, large-scale data over extensive temporal ranges. Although high-resolution imagery (e.g., less than 5 meters) can capture fine details, its limited availability, higher costs, and lower revisit frequencies reduce its utility for continuous, large-scale monitoring (Li et al., 2014; Sirko et al., 2023). Conversely, medium-resolution satellites such as Landsat and Sentinel-2 offer a balanced trade-off between spatial resolution and temporal coverage, with frequent revisit times and global availability. These characteristics make medium-resolution imagery particularly well-suited for near-real-time monitoring of gradual surface changes, including those driven by construction activities (Wulder et al., 2008).

However, construction activities represent a unique form of land disturbance, distinct from other processes like deforestation or agricultural expansion due to their multi-phase, recurring nature and long-lasting effects. Unlike other land-use conversions, construction transforms undeveloped areas into urban or industrial zones through multiple stages, such as vegetation removal, terrain modification, and the creation of impervious surfaces (Thornton et al., 2023). Each phase of construction generates unique spectral signatures in satellite imagery, making the detection and analysis of these activities more complex compared to uniform changes like forest clearing (Liu et al., 2021). Additionally, construction can occur in both urban and rural environments, further complicating its spatiotemporal monitoring (Schott et al., 2016).

Tracking construction activities using remote sensing poses unique challenges. Construction sites are often small, covering only a few pixels in medium-resolution imagery, which makes accurate change detection difficult (Huang et al., 2014; Sirko et al., 2023). The spectral diversity of materials like concrete, asphalt, and metal adds complexity, as different construction phases exhibit distinct spectral signatures (Kotthaus et al., 2014). This variability complicates using a single classification algorithm that can reliably detect all phases. Additionally, construction changes are often obscured by other land disturbances, such as urban expansion or natural vegetation cycles, requiring advanced algorithms to differentiate these signals. Unlike the more uniform changes associated with urban expansion, construction activities occur sporadically and involve rapid transformations in developed areas. This sporadic nature and the heterogeneity of materials across various sites and stages further complicate monitoring efforts.

To address these challenges, specialized algorithms have been developed for detecting land disturbances over time using satellite data, including the Continuous Change Detection and Classification (CCDC) algorithm (Zhu and Woodcock, 2014), Breaks for Additive Season and Trend (BFAST) (Almeida et al., 2018), and LandTrendr (Kennedy et al., 2010). These algorithms analyze temporal patterns in spectral data derived from dense time series, often sourced from medium-resolution satellites, to detect and classify land cover changes. Furthermore, the Continuous Monitoring of Land Disturbances (COLD) algorithm (Zhu et al., 2020) COLD algorithm excels in identifying "breaks" within time series data—points where significant land cover changes occur—enabling continuous disturbance monitoring across large areas (Suh et al., 2024).

Land use/land cover (LULC) studies often focus on broad categories, such as built-up areas or impervious surfaces, rather than specific activities like construction (Thornton et al., 2023). Consequently, construction activities are frequently subsumed under general urban expansion, making distinguishing construction from other urban growth or redevelopment forms challenging. Additionally, the relatively small spatial extent of many construction sites, combined with the medium resolution of satellite imagery, poses challenges for accurately classifying these areas in LULC datasets (Wang et al., 2023). This limitation highlights the need for more refined classification methods to differentiate construction activities from other types of land change. Current LULC classification schemes are typically too coarse to capture the distinct phases of construction, resulting in an underrepresentation of construction dynamics in large-scale land use studies. Given these challenges, applying the COLD algorithm is insufficient for monitoring construction activities, and relying solely on LULC data presents similar limitations.

In this study, we utilized the COLD algorithm on Harmonized Landsat and Sentinel (HLS) datasets to monitor construction activities in Egypt's New Capital. The COLD algorithm, known for detecting "breaks" in time series data, offers a robust framework for identifying land surface changes related to construction. By leveraging dense time series data from these satellites, we captured spatial and temporal breaks associated with ongoing construction, enabling continuous development monitoring in this rapidly expanding urban area. To further refine our detection process, we integrated publicly available LULC datasets from Esri with a 30-meter resolution to improve the classification of artificial surfaces. By overlaying the construction breaks detected by COLD with artificial surface data from the LULC datasets, we achieved enhanced classification accuracy for construction activities. We validated the proposed method by visually comparing it with high-resolution Google Earth imagery. The experiment results indicate a strong agreement between the detected breaks in the time series and observed construction progress, demonstrating the effectiveness of our approach in monitoring construction dynamics at a large scale.

The remainder of this paper is structured as follows: Section 2 outlines the materials and methods, detailing the study area, data datasets, and algorithms. Section 3 presents and discusses the results. Finally, Section 4 concludes the paper by highlighting key findings and suggesting future research directions.

2. Material and Methods

2.1 Study Area

This study focuses on New Cairo City and the New Administrative Capital, two regions in Egypt undergoing rapid urban development and large-scale construction. Figure 1 illustrates the spatial extent of the study area, emphasizing the urban boundaries and key regions of interest within both New Cairo City and the New Capital. In 2016, the Egyptian government launched the second development phase for New Cairo City and commenced the first construction phase for the New Administrative Capital. New Cairo City, situated southeast of Cairo, is an urban development project to alleviate congestion in the capital. The New Administrative Capital is located east of Cairo, a cornerstone of Egypt for a modern administrative hub. These regions arid desert climate, characterized by minimal vegetation and low cloud cover, makes it highly suitable for remote sensing-based analysis of construction changes. The total area encompasses approximately 1,000 square kilometers, extending between latitudes 29.8° and 30.0° N and longitudes 31.3° and 32.0° E.

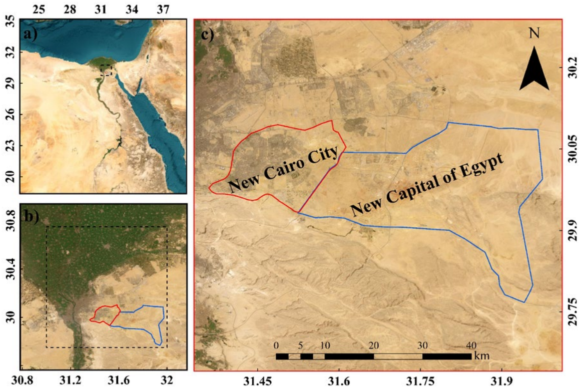

Figure 1. Geographic location of the study area. a) Geographic location of Egypt. b) Geographic location of the HLS tile (36RUU) represented by the dashed black rectangle. c) Geographic location of New Cairo City and the New Capital, surrounded by red and blue polygons, respectively.

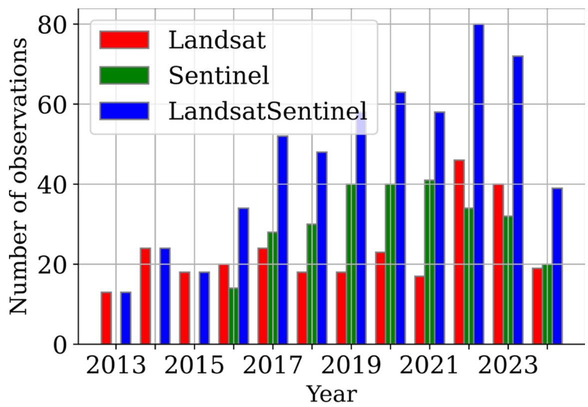

Figure 2. Data availability from the Harmonized Landsat and Sentinel (HLS) dataset based on a cloud coverage criterion of less than 5% spanning from July 1, 2013, to July 1, 2024.

2.2 Harmonized Landsat and Sentinel

The Harmonized Landsat and Sentinel (HLS) dataset (NASA, 2023), which integrates data from Landsat 8 and Sentinel-2, was employed to monitor construction activities in the study area. We utilized version 2.0 of the HLS dataset, which offers a spatial resolution of 30 meters. To enhance the temporal resolution of the dataset, a temporal consistency fusion of both satellite missions was performed, allowing for precise monitoring of land disturbance and construction-driven changes over time. To ensure optimal data quality, we applied a filtering process to select scenes with less than 5% cloud cover. Through the integration of Landsat-8 and Sentinel-2 observations, 559 near cloud-free images were acquired, spanning the period from July 1, 2013, to July 1, 2024. Figure 2 illustrates the temporal distribution of HLS scenes that met these criteria. These criteria provided a robust framework for capturing detailed and comprehensive spatial-temporal dynamics related to construction activities in New Cairo City and the New Administrative Capital. This multi-year analysis facilitated urban expansion and land transformation, tracking across the evolving landscape, demonstrating the utility of dense time series satellite data for continuous monitoring.

2.3 Land Use Land Cover

Numerous land use and land cover (LULC) datasets are available; however, many are constrained to data from 2019 or 2020. For this study, we selected the ESRI LULC dataset (ESRI, 2024), which offers a spatial resolution of 30 meters and a continuous time series spanning from 2017 to 2023. This extended temporal coverage is ideal for monitoring land use changes over time and aligns with the objectives of this study to assess ongoing urbanization processes. Figure 3 illustrates the LULC changes across the same spatial extent as the HLS tile, maintaining matching spatial resolution. The time series analysis of the LULC dataset reveals a substantial increase in built-up areas, consistent with the development plan to establish new urban centers in East Cairo, including New Cairo City and the New Administrative Capital.

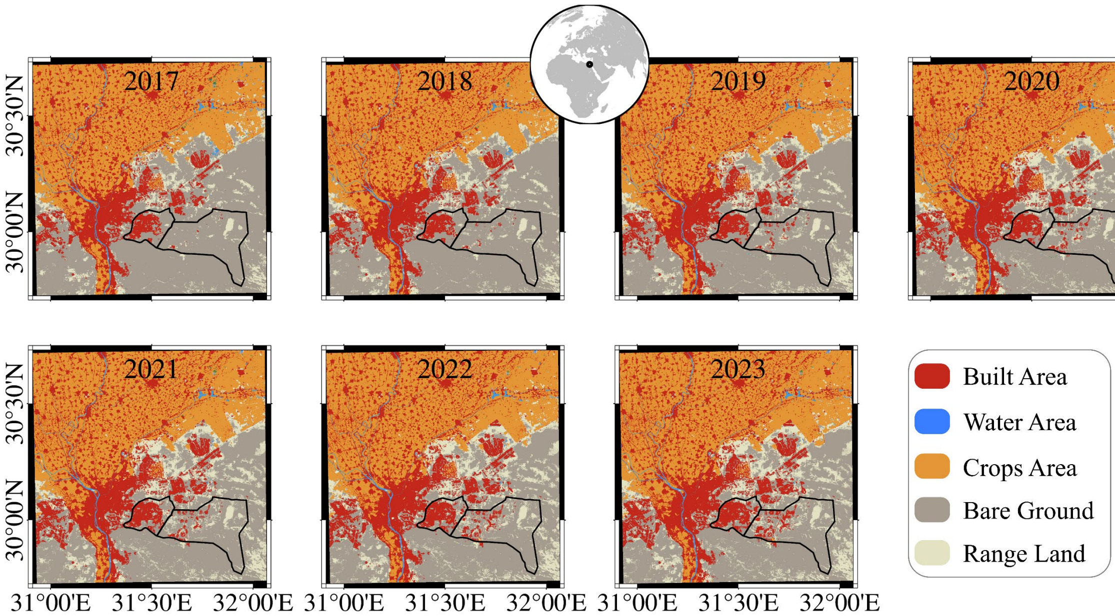

Figure 3. Time series of land use and land cover (LULC) extracted from the ESRI dataset from 2017 to 2023.

2.4 Land Disturbance

The Continuous Monitoring of Land Disturbance (COLD) algorithm (Zhu et al., 2020), implemented in Python (GERSL, 2022), analyzes satellite imagery to detect breaks in surface reflectance, signifying disturbances, or recovery events. These breaks are caused by construction activities, land clearing, or afforestation and can be identified by comparing successive observations with the time series model output. The formula used by the COLD algorithm is a combination of constant, linear, and periodic trends that can be expressed as follows:

$$\hat{\rho}_{(i,x)} = a_{(i,0)} + \sum_{k=1}^{3} \left\{ a_{(i,k)} \cos\left(\frac{2\pi}{T}x\right) + b_{(i,k)} \sin\left(\frac{2\pi}{T}x\right) \right\} + c_{(i,1)}x \quad (1)$$

where x represents the Julian date, i donates the ith band, and T is the number of days in a year. The term $a_{(i,0)}$ corresponds to the constant coefficient for the ith band, while $a_{(i,k)}$ and $b_{(i,k)}$ are coefficients representing intra-annual periodic changes for the ith band. Additionally, $c_{(i,1)}$ is the coefficient for intra-annual linear changes (slope) for the ith band and $\hat{\rho}_{(i,x)}$ signifies the predicted value for the ith band at the date x.

As shown in Figure 4, the COLD algorithm effectively represents land disturbance in a spatiotemporal context by pinpointing individual pixel breaks in the temporal profile. Figure 4(a) indicates the temporal profile for the pixel located at (30.912° E, 30.716° N), revealing a break identified on December 25, 2016. In contrast, Figure 4(b) presents the temporal profile for the pixel located at (30.938° E, 30.716° N), which displays three breaks identified on March 24, 2020; November 14, 2021; and January 19, 2023.

The COLD algorithm has been cross-validated with high-resolution imagery to ensure accuracy in detecting and quantifying construction-induced land disturbances (Suh et al., 2024). This technique is particularly well-suited for large-scale, ongoing construction projects, such as those in New Cairo City and the New Capital, where development occurs at varying rates across different zones. By applying the COLD algorithm, we can continuously monitor urban areas, enabling a detailed temporal assessment of urban sprawl and construction growth.

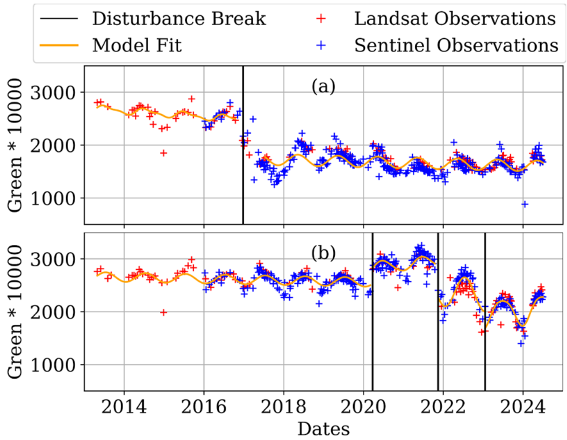

Figure 4. Visualization of land breaks extracted from the COLD time series algorithm. (a) Temporal profile for the pixel located at (30.912° E, 30.716° N). (b) Temporal profile for the pixel at (30.938° E, 30.716° N). The vertical black lines denote break events.

2.5 Construction Change

The detection and quantification of construction changes are conducted through a three-stage process, as illustrated in Figure 5: (a) Estimating the time series of land disturbance breaks using the COLD algorithm, (b) Extracting the time series of artificial surfaces from LULC data, and (c) Determining the subset of construction changes by intersecting the land disturbance breaks with the artificial surface data.

To identify and quantify land disturbances, we employed the COLD algorithm. This algorithm segments the spatiotemporal HLS data into small blocks and applies a time series model to the satellite observations of each pixel. Utilizing the red, green, blue, NIR, SWIR1, and SWIR2 bands, it detects land disturbances and change vectors in spatiotemporal maps by reconnecting the small blocks. The LULC time series data were utilized to extract artificial surfaces by categorizing built-up areas while grouping all other categories as background. To accurately capture construction changes, we concentrated on land disturbances within the defined urban development boundaries established by artificial surface extraction. Any land disturbance occurring within these boundaries is classified as a construction change. By intersecting land disturbances from one year with the urban development boundaries from the subsequent year, we can identify construction activities that transpired during the intervening period. This way, the proposed method can precisely track annual construction progress as new areas are disturbed and transformed into urban infrastructure.

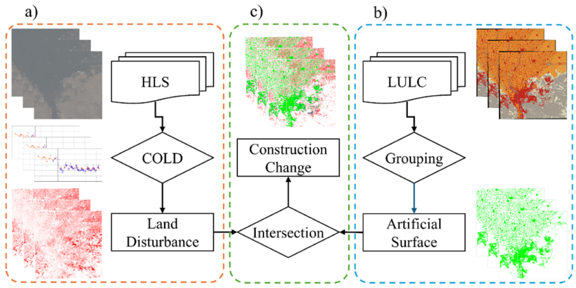

Figure 5. The proposed methodology for construction dynamics monitoring. a) HLS time series processing workflow. b) LULC time series processing workflow. c) Intersection between land disturbance time series and artificial surfaces time series.

3. Results and discussions

3.1 Artificial Surfaces Time Series

The LULC from ESRI provides a temporal evolution of the overall urban development in the study area, as shown in Figure 6. In 2017, the artificial surfaces were approximately zero in the New Administrative Capital, revealing the preconstruction activities of the last year. The time series of artificial surfaces from 2017 to 2023 shows a significant increase consistently with the urban development of the first phase of the New Administrative Capital.

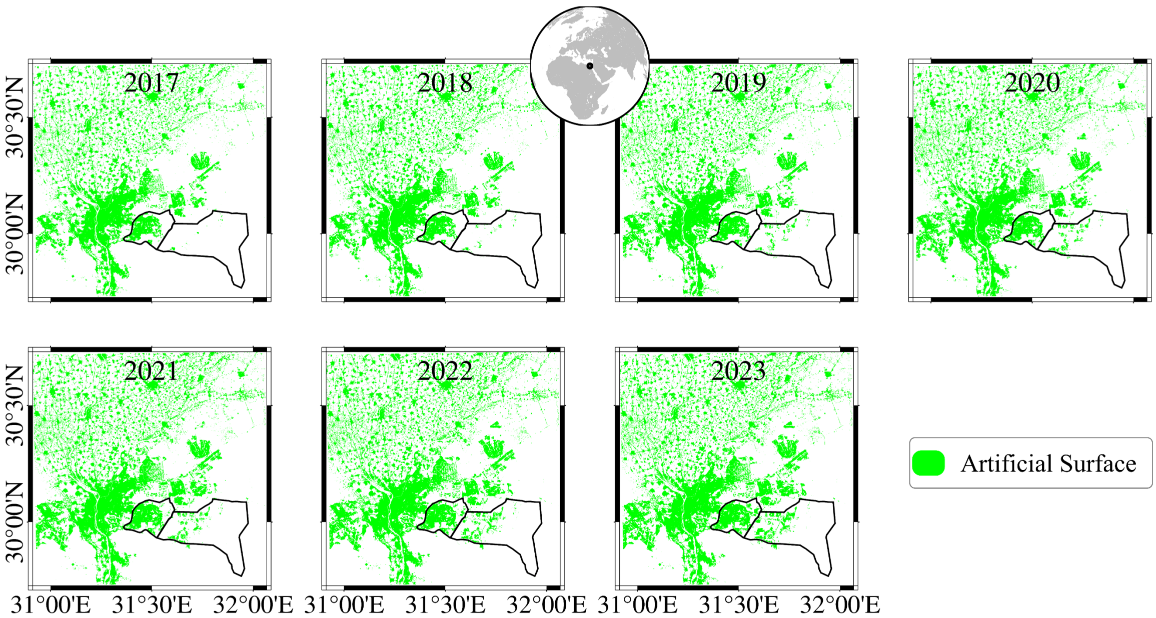

Figure 6. Time series of the artificial surface grouped from the LULC.

3.2 Land Disturbance Time Series

The COLD algorithm effectively detected spatiotemporal land disturbances across the study area, as shown in Figure 7. Between 2013 and 2016, the number of identified disturbances remained relatively low, mainly due to the limited frequency of satellite observations, as this period relied solely on Landsat data. This finding is further supported by the fact that New Cairo City and the New Capital exhibited no significant land disturbances during this timeframe, as major construction activities had not yet begun. Starting in 2016, a marked increase in land disturbances was observed, correlating with the initiation of significant construction efforts. These early disturbances predominantly involved excavation, land leveling, and other pre-construction activities and are not classified as built-up areas (see Figure 6). The sharp rise in disturbances signifies the preparatory phase of large-scale urban development, signaling the transition from undeveloped land to urbanized infrastructure.

Outside the defined urban development boundaries, land disturbances were primarily linked to agricultural land encroachment, which is strictly regulated under Egyptian law. Additionally, substantial disturbances were observed in the northeastern portion of the study area, where land reclamation projects aimed at expanding agricultural lands were undertaken—a key initiative by the Egyptian government to increase arable land for cultivation.

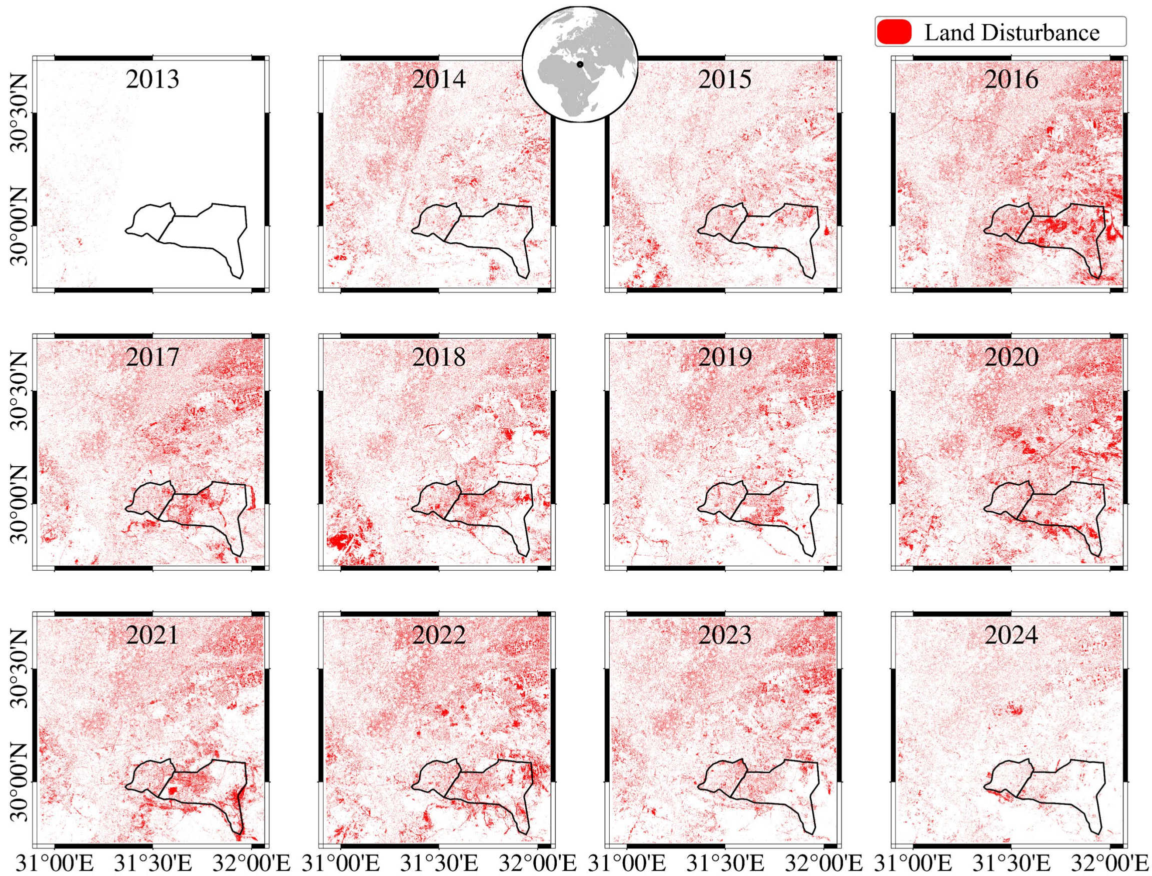

Figure 7. The spatiotemporal time series of land disturbance calculated from the COLD algorithm.

3.3 Construction Change Time Series

We concentrate on land disturbances within urban development boundaries, emphasizing the importance of utilizing an accurate and current LULC dataset. While Figure 6 shows a general increase in artificial surface areas over time, it potentially underestimates the true extent of built-up regions, as suggested by the broader land disturbances detected in Figure 7. These disturbances include construction activities such as foundational work, which may not have been classified as artificial surfaces in Figure 6. To mitigate this discrepancy, we utilize artificial surface data from the subsequent year, which typically provides a more accurate representation of newly developed areas (Suh et al., 2024). This time-lag approach helps to better correlate land disturbances with construction activities. Figures 8 and 9 display the intersection between artificial surfaces (in green) and land disturbances (in red), highlighting areas of construction change (in blue), using the same year data and a year difference data, respectively. Figure 9 shows a little increase in the construction area, depending on a lot of land disturbance leading to artificial surfaces in the consecutive year. In Figure 10, the cumulative areas of other artificial surfaces, other land disturbances, and construction changes are presented for the entire tile. Figure 10 (a) depicts the year-by-year intersection of artificial surfaces and land disturbances, while Figure 10 (b) illustrates the intersection between artificial surfaces and land disturbances from the previous year. The latter method, shown in Figure 10 (b), captures a similar pattern but with a slight increase in the area classified as construction change, offering a more accurate portrayal of the progression of urban development over time. The construction changes range from 18.3×10^3 to 27.4×10^3 square meters annually.

https://doi.org/10.5194/isprs-annals-X-G-2025-3-2025

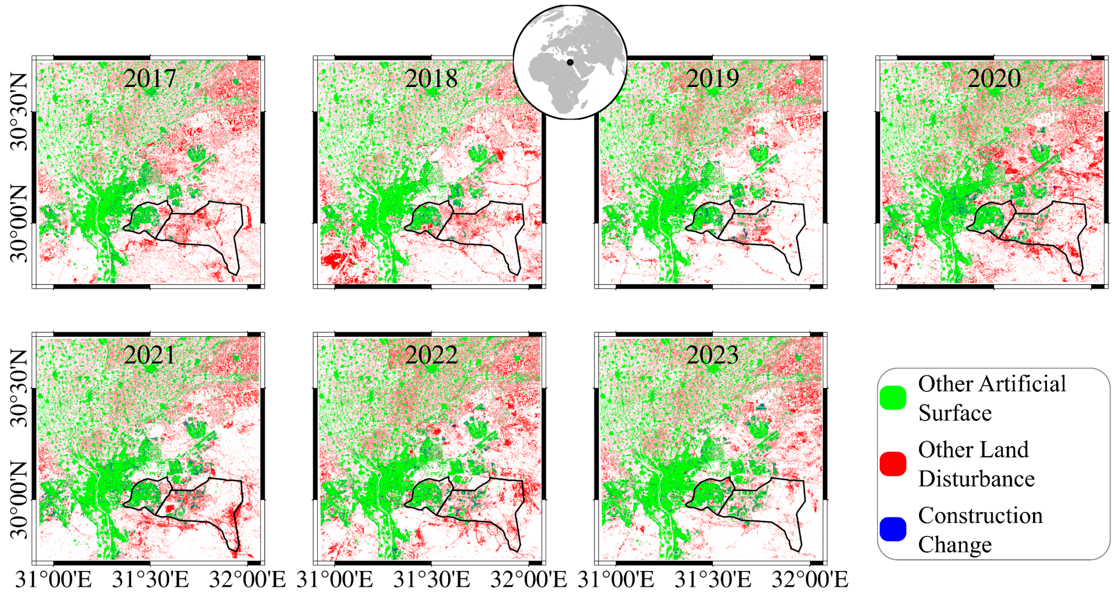

Figure 8. Time series of construction changes calculated by intersecting artificial surfaces and land disturbances in the same year.

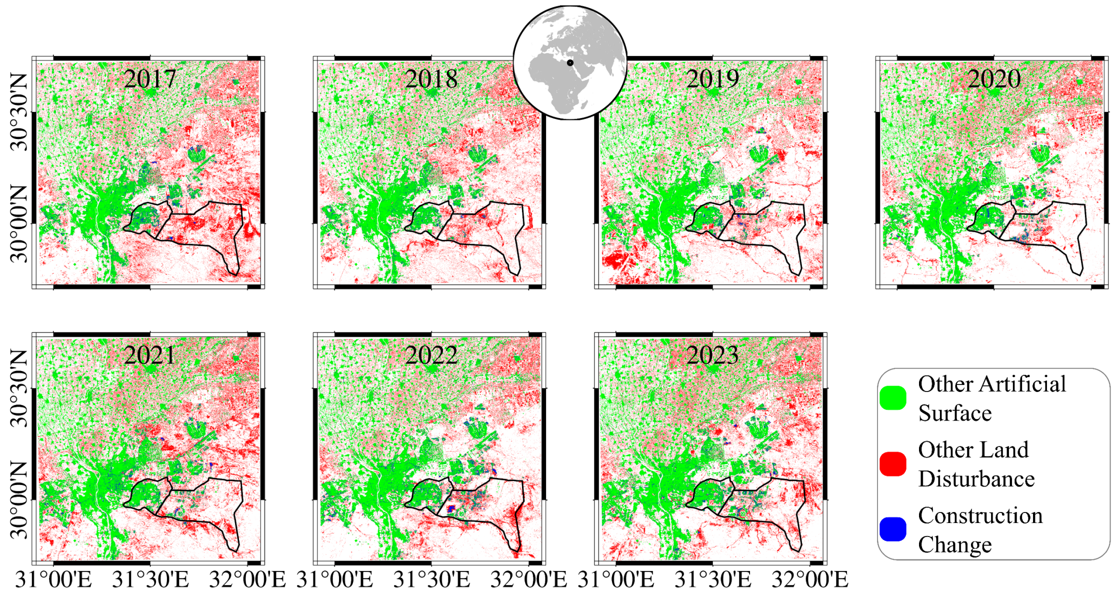

Figure 9. Time series of construction changes calculated by intersecting artificial surfaces and land disturbances from the previous year.

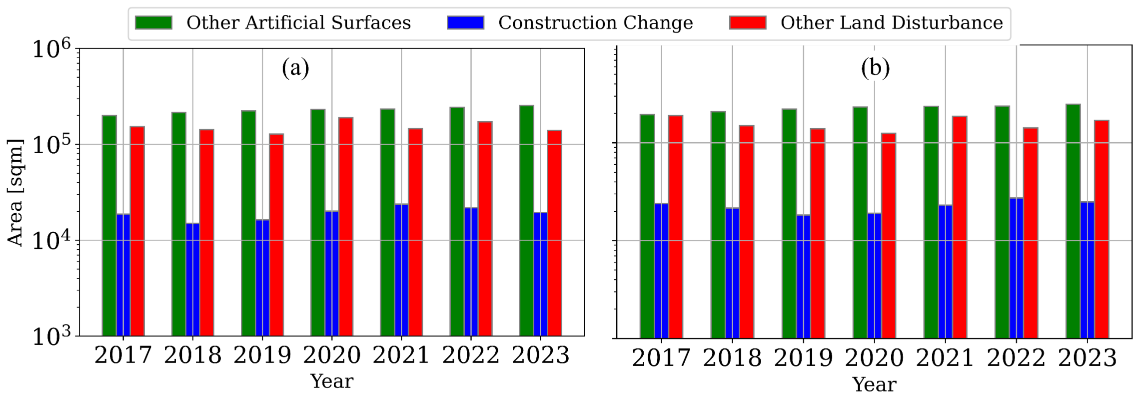

Figure 10. Area changes associated with different land disturbances: (a) The intersection of artificial surfaces and land disturbances within the same year, as depicted in Figure 8. (b) The intersection of artificial surfaces with land disturbances from the previous year, as illustrated in Figure 9. All dates correspond to the land cover dataset, reflecting the timing of land surface classification updates.

https://doi.org/10.5194/isprs-annals-X-G-2025-3-2025 | © Author(s) 2025. CC BY 4.0 License.

3.4 Validation

To visually validate the proposed method, as shown in Figure 11, we obtained a time series of high-resolution imagery from Google Earth and overlaid it with the intersection of artificial surfaces and land disturbances from the previous year. Figure 11 (a) highlights the preconstruction activities, such as excavation and land leveling, where land disturbance is at its peak. As artificial surfaces expand, this region transitions from disturbed land into an urbanized area. Figure 11 (d) shows significant construction activities in the octagon area, marked by the black circle, indicating the extensive construction activities. In Figure 11 (f), numerous completed construction activities are visible, transformed into artificial surfaces, as shown in Figure 11 (g). This progression illustrates the evolution of initially disturbed areas into built environments, consistent with observed patterns of urban expansion. The overlay of high-resolution imagery with the detected land disturbances and artificial surfaces effectively validates the accuracy of the proposed method. The comparison results confirmed that the temporal and spatial patterns of construction change closely match real-world observations.

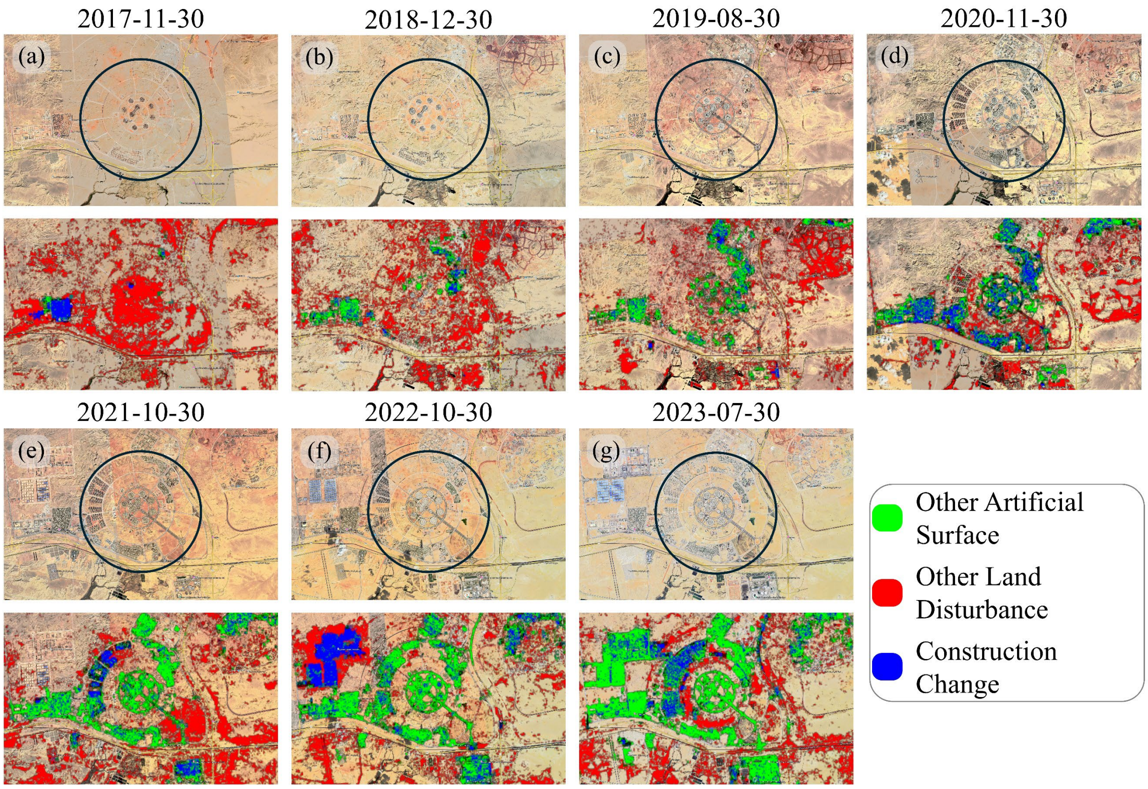

Figure 11. Time series of Google high-resolution images over the Octagon (Egyptian Ministry of Defense) based on 9. The black circle denotes the octagonal area.

4. Conclusions

We proposed an enhanced COLD procedure to monitor the land disturbances for change detection. This method jointly utilized the HLS and the publicly available LULC datasets to track construction activities in rapidly developing areas. We take the new capital city of Egypt as the study area. By applying the COLD algorithm to Landsat and Sentinel-2 data, we effectively identified breaks in land disturbance and tracked construction progress from 2016 to the present. Integrating LULC maps with COLD breaks revealed the spatial-temporal development patterns and allowed for a refined classification of construction changes. Both overlapping analyses produced similar results using LULC maps of the same year and subsequent year. The latter method provided a slightly more comprehensive depiction of construction expansion, highlighting its utility in providing a more accurate picture of development over time. The comparison of satellite-based results with historical Google Earth imagery confirmed the robustness of this methodology for continuous construction monitoring. The experiment results demonstrate that the proposed approach can offer a scalable, cost-effective method for detecting and analyzing land-use changes in other regions, contingent upon the availability of time series data and LULC maps.

The limitations of this study are primarily associated with three key factors: (1) the temporal scope of the time series data, (2) the accuracy of detected artificial surfaces, and (3) the spatial resolution of the datasets used. The ESRI LULC dataset spans from 2017 to 2023, restricting our analysis of artificial surface dynamics outside this period and consequently limiting insights into urban development trends from 2013 to 2016. The accuracy of artificial surface classification is critical for precisely delineating urban development boundaries; misclassifications may result in inaccurate representations of construction activities and urban expansion, which could skew the study’s findings. Furthermore, the 30-meter spatial resolution of the data may be inadequate for detecting small-scale construction activities, particularly in densely developed areas, thereby impeding detailed assessments of urban growth and fine-scale construction changes.

To overcome these limitations, future work will focus on the following strategies: First, to extend the analysis to the 2013-2016 period, deep learning-based methods will be explored for reconstructing artificial surfaces and urban development patterns. These approaches could provide more consistent and accurate temporal coverage, enabling a continuous analysis of land disturbances over a longer timeframe. Improving the accuracy of artificial surface detection will be a priority, integrating higher-resolution imagery to enhance the delineation of urban boundaries and refine the interpretation of construction activities. Additionally, leveraging higher-resolution satellite imagery will facilitate the detection of smaller construction sites, allowing for a more detailed examination of urban growth trajectories and construction progress. This will significantly benefit rapidly developing areas like New Cairo City and the New Capital, providing deeper insights into urban dynamics and development patterns.

Acknowledgements

The research was jointly supported by the Research Grants Council (RGC) of the Hong Kong Special Administrative Region (Grants No. 152318/22, 152344/23), the National Natural Science Foundation of China (Grants No. 42330717), and the University Grants Council of the Hong Kong Polytechnic University (Grants No. P0045896).

References

Almeida, A.E., Menini, N., Verbesselt, J., De Torres, R.S., 2018. BFast Explorer: An effective tool for time series analysis. *International Geoscience and Remote Sensing Symposium (IGARSS)*, 2018-July, 4913–4916. https://doi.org/10.1109/IGARSS.2018.8517877

ESRI, 2024. Esri Land Cover Explorer [WWW Document]. URL https://livingatlas.arcgis.com/landcoverexplorer (accessed 10.1.24).

Friedl, M.A., McIver, D.K., Hodges, J.C.F., Zhang, X.Y., Muchoney, D., Strahler, A.H., Woodcock, C.E., Gopal, S., Schneider, A., Cooper, A., Baccini, A., Gao, F., Schaaf, C., 2002. Global land cover mapping from MODIS: Algorithms and early results. *Remote Sensing of Environment*, 83, 287–302. https://doi.org/10.1016/S0034-4257(02)00078-0

GERSL, 2022. PyCOLD [WWW Document]. URL https://github.com/GERSL/pycold (accessed 7.1.24).

Huang, X., Zhang, L., Zhu, T., 2014. Building change detection from multitemporal high-resolution remotely sensed images based on a morphological building index. *IEEE Journal of Selected Topics in Applied Earth Observations and Remote Sensing*, 7, 105–115. https://doi.org/10.1109/JSTARS.2013.2252423

Kennedy, R.E., Yang, Z., Cohen, W.B., 2010. Detecting trends in forest disturbance and recovery using yearly Landsat time series: 1. LandTrendr - Temporal segmentation algorithms. *Remote Sensing of Environment*, 114, 2897–2910. https://doi.org/10.1016/j.rse.2010.07.008

Kotthaus, S., Smith, T.E.L., Wooster, M.J., Grimmond, C.S.B., 2014. Derivation of an urban materials spectral library through emittance and reflectance spectroscopy. *ISPRS Journal of Photogrammetry and Remote Sensing*, 94, 194–212. https://doi.org/10.1016/j.isprsjprs.2014.05.005

Li, D., Bou-Zeid, E., Oppenheimer, M., 2014. The effectiveness of cool and green roofs as urban heat island mitigation strategies. *Environmental Research Letters*, 9. https://doi.org/10.1088/1748-9326/9/5/055002

Liu, T., Yang, L., Lunga, D., 2021. Change detection using deep learning approach with object-based image analysis. *Remote Sensing of Environment*, 256, 112308. https://doi.org/10.1016/j.rse.2021.112308

NASA, 2023. Harmonized Landsat Sentinel [WWW Document]. URL https://hls.gsfc.nasa.gov/ (accessed 7.1.24).

Schott, J.R., Gerace, A., Woodcock, C.E., Wang, S., Zhu, Z., Wynne, R.H., Blinn, C.E., 2016. The impact of improved signal-to-noise ratios on algorithm performance: Case studies for Landsat class instruments. *Remote Sensing of Environment*, 185, 37–45. https://doi.org/10.1016/j.rse.2016.04.015

Sirko, W., Brempong, E.A., Marcos, J.T.C., Annkah, A., Korme, A., Hassen, M.A., Sapkota, K., Shekel, T., Diack, A., Nevo, S., Hickey, J., Quinn, J., 2023. High-Resolution Building and Road Detection from Sentinel-2 1–25.

Suh, J.W., Zhu, Z., Zhao, Y., 2024. Monitoring construction changes using dense satellite time series and deep learning. *Remote Sensing of Environment*, 309, 114207. https://doi.org/10.1016/j.rse.2024.114207

Thornton, P.E., Reed, B.C., Xian, G.Z., Chini, L., East, A.E., Field, J.L., Hoover, C.M., Poulter, B., Reed, S.C., Wang, G., Zhu, Z., 2023. Land cover and land-use change, in: Crimmins, A.R., Avery, C.W., Easterling, D.R., Kunkel, K.E., Stewart, B.C., Maycock, T.K. (Eds.), Fifth National Climate Assessment. U.S. Global Change Research Program, Washington, DC, USA. https://doi.org/10.7930/NCA5.2023.CH6

United Nations, 2022. Population [WWW Document]. URL https://www.un.org/en/ global-issues/population (accessed 10.1.24).

Wang, Y., Sun, Y., Cao, X., Wang, Y., Zhang, W., Cheng, X., 2023. A review of regional and Global scale Land Use/Land Cover (LULC) mapping products generated from satellite remote sensing. *ISPRS Journal of Photogrammetry and Remote Sensing*, 206, 311–334. https://doi.org/10.1016/j.isprsjprs.2023.11.014

Winkler, K., Fuchs, R., Rounsevell, M., Herold, M., 2021. Global land use changes are four times greater than previously estimated. *Nature Communications*, 12, 1–10. https://doi.org/10.1038/s41467-021-22702-2

Wulder, M.A., White, J.C., Goward, S.N., Masek, J.G., Irons, J.R., Herold, M., Cohen, W.B., Loveland, T.R., Woodcock, C.E., 2008. Landsat continuity: Issues and opportunities for land cover monitoring. *Remote Sensing of Environment*, 112, 955–969. https://doi.org/10.1016/j.rse.2007.07.004

Zhu, Z., Woodcock, C.E., 2014. Continuous change detection and classification of land cover using all available Landsat data. *Remote Sensing of Environment*, 144, 152–171. https://doi.org/10.1016/j.rse.2014.01.011

Zhu, Z., Zhang, J., Yang, Z., Aljaddani, A.H., Cohen, W.B., Qiu, S., Zhou, C., 2020. Continuous monitoring of land disturbance based on Landsat time series. *Remote Sensing of Environment*, 238, 111116. https://doi.org/10.1016/j.rse.2019.03.009